

Low Latency DESDynI Data Products for Disaster Response, Resource Management and Other Applications

J. Doubleday¹, S. Chien¹, Y. Lou¹

¹Jet Propulsion Laboratory, 4800 Oak Grove Drive, Pasadena, CA 91101
(joshua.r.doubleday, steve.a.chien, Yunling.Lou)¹@jpl.nasa.gov

Abstract – We are developing onboard processor technology targeted at the L-band SAR instrument onboard the planned DESDynI mission to enable formation of SAR images onboard opening possibilities for near-real-time data products to augment full data streams. Several image processing and/or interpretation techniques are being explored as possible direct-broadcast products for use by agencies in need of low-latency data, responsible for disaster mitigation and assessment, resource management, agricultural development, shipping, etc. Data collected through UAVSAR (L-band) serves as surrogate to the future DESDynI instrument. We have explored surface water extent as a tool for flooding response, and disturbance images on polarimetric backscatter of repeat pass imagery potentially useful for structural collapse (earthquake), mud/land/debris-slides etc. We have also explored building vegetation and snow/ice classifiers, via support vector machines utilizing quad-pol backscatter, cross-pol phase, and a number of derivatives (radar vegetation index, dielectric estimates, etc.). We share our qualitative and quantitative results thus far.

Keywords: realtime, SAR, polarimetry, classification, disaster management, onboard processing, applications

1. INTRODUCTION

The planned Deformation, Ecosystem Structure and Dynamics of Ice (DESDynI) mission would collect an enormous amount of data using a repeat pass Interferometric Synthetic Aperture Radar operating at 1.2 GHz (L-Band) and full polarimetric mode, generating images of resolution better than 10m pixels over swaths 240km in range (Desdyni 2011). For many years to come this data should prove valuable to scientific research with respect in areas improving our understanding of earthquakes, volcanic activity, landslides, dynamics of ice-sheets in our rapidly changing environment and how our climate is interrelated with terrestrial biomass. In the short term, these same data could have immediate utility for disaster management, resource management, and other agencies working within time restrictions and data-processing limitations. For example an invaluable tool for emergency responders in a flood situation would be a surface water extent map.

As an associated piece of this work, JPL has developed a hardware approach for processing raw polarimetric L-band SAR data based on Xilinx Virtex series FPGA (Lou 2010). This has been deployed on the Uninhabited Aerial Vehicle Synthetic Aperture Radar (UAVSAR), an airborne radar system typically flying at altitudes of ~14000 meters along a computer controlled flight tube of 10m diameter while electronically steering a L-band radar, generating images of nearly 2m resolution before

multilooking (UAVSAR 2010). The hardware processor is designed to be compatible with both UAVSAR and the radar proposed in DESDynI, allowing SAR image formation of 10m resolution in near-real-time, and subsequent analysis on those data.

We have identified several applications areas to explore data processing and classification results under conditions feasible for a space-borne platform: surface water extent mapping for flood applications, coarse vegetation classification for resource management and/or fire monitoring, snow/ice/land classification for transportation management or water resource management and finally repeat-pass disturbance processing for landslide mitigation and monitoring.

In each of these applications latency between data acquisition and delivery, and actual coverage of region-of-interest are of the utmost important to the end-user. DESDynI's future mission would be downlink constrained; onboard processing could condense these data through image formation and classification, allowing for urgent and last minute requests that would otherwise not fit in the schedule. Onboard processing coupled with direct-broadcast could further alleviate latency.

2.1 REPEAT PASS DISTURBANCE DETECTION

Our first and possibly simplest product presented here is a simple composite of radar backscatter returned between two scenes on a 0-baseline. This is intended as a tool for an expert familiar with radar signatures to identify expanses of disturbance or change over the temporal baseline.

UAVSAR collected data along the San Gabriel Mountain range both in February 2009 and September 2009 using the same flight path to within 10 meters accuracy, covering portions of the Angeles National Forest which suffered the 160,000 acre fire from late August 2009 through October 2009, costing \$95 million in containment (USDA 2009). In Figure 1 backscatter image data from the initial flight has been used to color red intensity, while blue/green used to color the later flight. Figure 2 shows the same data, but with differences of 3dB or more highlighted red/green for vegetated/non-veg areas (prior to burn). Figure 3 shows a burn scar image generated from ASTER data acquired September 6th, 2009, with an approximate outline of the UAVSAR data product (Allen 2009).

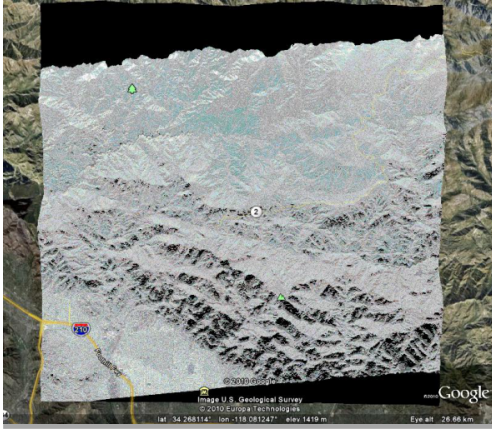


Figure 1. Composite of repeat-pass HH backscatter images from Feb. 2009 (blue) and Sept. 2009 (red)

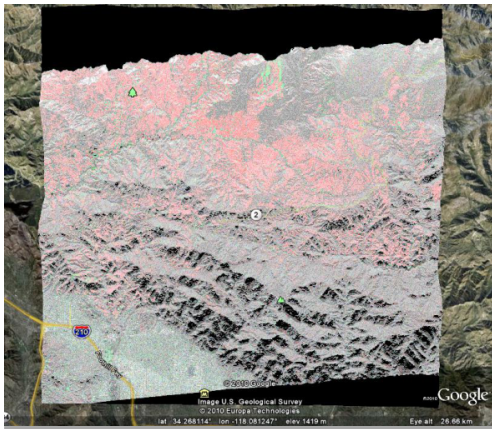


Figure 2. Repeat pass change in backscatter >3db. Red for vegetated areas (NLCD2001) and green for non-vegetated.

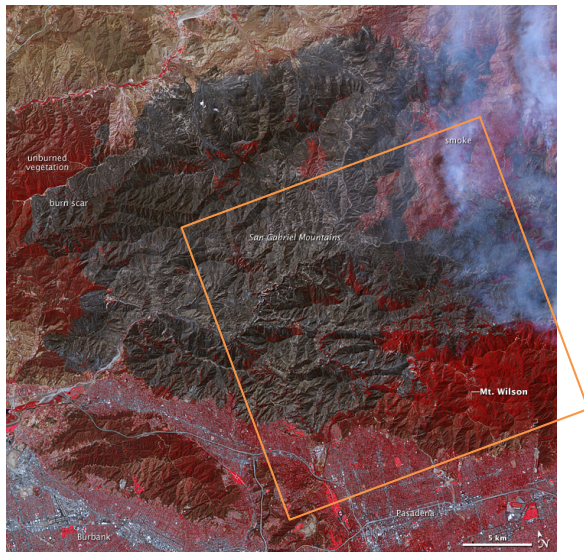


Figure 3. ASTER image enhanced to contrast vegetation (red) and fire-scar (black/grey) (Allen 2009).

In comparing Figure 2 and 3, distinguishable areas with remaining vegetation as seen in the ASTER data coincide well with regions of non-disturbance in the UAVSAR composite image (e.g. see ‘boot-like’ feature top-center of Figure 2). We have no quantitative results to post at this time but have other examples, such as wetland drainage, and hope to generate similar results for landslides and urban disturbance (Haiti).

2.2 SURFACE WATER EXTENT

Our next algorithm is slightly more complex in-so-far as analysis is concerned when compared to the disturbance images discussed above, but requires only a single overpass of data to generate its estimation of surface water extent mask.

Water’s strong dielectric constant is rarely seen on the earth’s surface by other materials of common abundance (i.e. entire 10m x 10m pixel areas) and thus makes it a good quantity for classification. We use empirical estimations of the dielectric constant from polarimetric backscatter returns as reported by (Dubois 1995) and approximated with equation 1 where θ is the local incident angle and λ is the radar wavelength in cm:

$$\frac{\sigma_{hh}}{\sigma_{vv}} = \frac{14 \sin^2 \theta - 11 \cos^2 \theta}{\sin^2 \theta - 26.5 - 100 \log_{10}(\cos 2.55 \sin 1.3 \lambda \tan \theta)}$$

(1)

We also used filtering for vegetated areas (and thus inapplicable for the dielectric estimation by eq. 1) pixels with $\frac{\sigma_{hh}}{\sigma_{vv}} > -11 \cos^2 \theta$. Experimentation of varying a dielectric threshold to classify water vs non-water yielded a good threshold of 15. As a proxy for surface water as seen in a flood, we have used the water class of NLCD2001 land cover data (US.EPA 2011) in estimating this threshold and generating cross validation results. Table 1 summarizes results in a confusion matrix as generated from applying this algorithm to approximately 10 scenes of UAVSAR data collected over the Florida Everglades on June 16 2009.

Table 1. Classification breakdown of surface water extent classifier, vs NLCD2001 data.

NLCD		Classified: not water	water	count
wetland	woody	98%	2%	41509483
water		19%	81%	17490057
wetland	emergent herbaceous	91%	9%	11799208
urban	open space	99%	1%	77507
urban	cleared	96%	4%	69834
forest	evergreen	100%	0%	46719
urban	moderate intens	96%	4%	14897
low	barren land	64%	36%	11444
urban	intense	93%	7%	1928
low	grassland	87%	13%	1581

While fairly precise accuracies are achieved against the woody-wetland class, the dominant class in the region of our study, the

water class shows significant false negatives that we suspect are the result of surface roughness effects (Bragg scattering), a component left unaccounted for in our dielectric estimation. Figure 4 is an example of such a classification map, largely correct, but with some streaks of these false negatives in the open water region. Future work may include effort to characterize conditions for this misclassification and/or whether this effect is relevant to actual flooding scenarios.

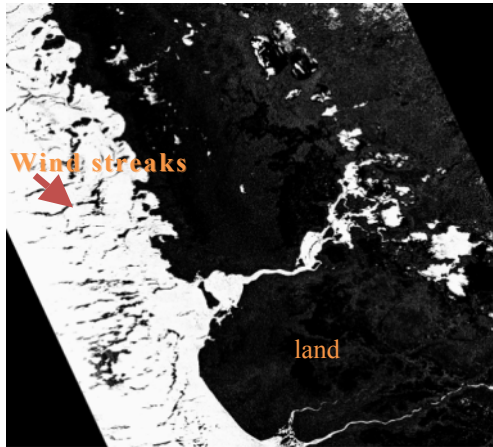


Figure 4. Surface water extent map of Florida Everglades. White: water, black: non-water Dark streaks on left are false negatives (assumed from surface roughening from wind).

2.3 VEGETATION CLASSIFICATION

The feasibility of generating a vegetation classification scheme using our real-time L-band SAR data has been studied using a multi-class support vector machine (SVM). Using UAVSAR data collected over forested and wetland areas of Maine and Vermont, spread out over approximately 12 days of varying weather, we trained a support vector machine using land cover maps from NLCD2001 with classes collapsed down to 7 coarser vegetation classes: dense (forest), herbaceous wetland, forested wetland, medium (shrub), low (grass), bare land and water. Approximately 5000 training samples (pixels) were chosen at random across the Maine dataset and included features of backscatter for HH, VV, HV, HHVV phase, 7x7 pixel averages

Table 2. Confusion matrix for vegetation classification vs NLCD2001 condensed classes, evaluated over ~15 30kmx30km images from Maine and Vermont

NLCD		Classifier results:							count
		1000	2000	2100	2200	3000	4000		
water	1000	54%	4%	2%	19%	11%	10%	682,069	
dense veg (forest)	2000	0%	45%	21%	12%	11%	10%	16,382,691	
wetland (herbaceous)	2100	1%	31%	30%	17%	12%	10%	1,936,352	
wetland (woody)	2200	6%	18%	17%	24%	17%	19%	478,129	
moderate veg (shrub)	3000	3%	25%	15%	13%	20%	23%	450,214	
light veg (grass)	4000	8%	19%	10%	18%	19%	25%	51,743	
urban	5000	5%	16%	8%	27%	23%	21%	323,258	
urban (low intensity)	5100	6%	19%	9%	21%	22%	22%	519,914	
developed (open space)	5200	3%	28%	13%	16%	20%	20%	775,630	
Total Accuracy:		8668968 / 19981198 (0.433856)							

and variance of some of these quantities for 19 total features. Training yielded ~900 support vectors using a Gaussian radial basis kernel.

Table 2 shows fairly poor classification performance when compared against NLCD2001 data, with the best accuracy at 54% for the water class of which 19% were misclassified as woody wetland, while dense vegetation had the next best accuracy of 46%, with 21% misclassified as herbaceous wetland. These figures are fairly underwhelming, however qualitative inspection of results look more promising and draw doubt upon our validation set. Figures 5a and 5b show the contrast in NLCD2001 ground truth to classifier output, while optical imagery in figure 5c shows a better visual correlation with the classifier output – of note is the abundance of light vegetation (open spaces or grassy areas, brown) consistent with the output, opposed to the majority of dense forest indicated in the ground truth in figure 5a. We suspect the NLCD2001 data is ultimately too noisy for training and validation purposes either because of age, resolution/aliasing artifacts (NLCD2001 is 30m resolution while UAVSAR is better than 10m allowing for individual tree crown identification) or other general fidelity problems. Future work will identify better land cover data and investigate improvements in cross-validation, while at the moment we find it interesting that with this potentially noisy dataset we obtain results that compare well, at least qualitatively with more recent optical data.

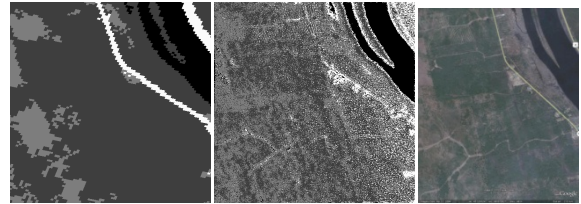


Figure 5. Vegetation classification data for scene in Maine, collected Sept 2009. (a) NLCD2001 land cover map, (b) classification results, (c) optical imagery courtesy Google Earth. Color scheme for (a) and (b), black: water, dark-gray: dense veg (including wetlands), gray: moderate veg, light-gray: light-veg, white: developed areas

Finally we would note that the resulting SVM, with ~900 support vectors would be too complex to be run on an in-flight platform. We anticipate replacing noisy training data with more accurate data would result in a reduced set and better cross-validation results. Other approaches to reach a feasible computation time would include a hardware based SVM evaluator or reduced set SVM (Tang 2006) or progressive SVMs (Wagstaff 2010).

2.4 SNOW/ICE CLASSIFICATION

We again employ a support vector machine to classify pixels of ground projected data using the same feature set as presented in section 2.3 for vegetation classification, but with target classes of snow or ice versus land versus water. Data collected over Iceland's Hofsjokull on Jun 12th 2009 together with various optical remote sensing data including Landsat7 taken May 16 2009 (Figure 6a) to serve as our training and validation data, and ground truth. Given the time of year, and large temporal

separation between the optical and UAVSAR data collection, we generated a conservative hand labeled training and validation set (Figure 6b), taking into consideration late-summer data to find a year-round snow pack. Training on ~300 randomly sampled pixels from the hand-labeled set resulted in the classification image of Figure 7, and the confusion matrix in Table 3.

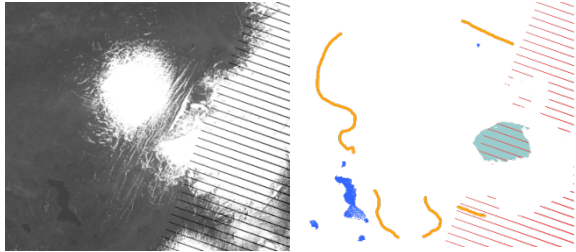


Figure 6. On left (a) Landsat7 band 1 image collected 2009-05-16, snow and ice from Hofsjokul on right, and seasonal snow on volcanic peak at center top. On right (b) is a conservative hand-labeling, water: blue, land: orange, snow/ice: gray, red: no-data.



Figure 7. Result of Snow/Ice SVM classifier: pink: land, dark-gray: water, gray-blue: snow/ice

Table 3. Confusion matrix of snow/ice classifier against hand labels, data collected Jun 12th 2009.

	water	ice	land	count
no label	7%	10%	83%	16.7M
water	91%	3%	6%	145884
ice	3%	90%	7%	440706
land	1%	2%	96%	311201
Total Accuracy: 829007 / 897791 (0.923385)				

Overall classification accuracies (>90%) are much improved as compared to the vegetation classifier and the number of support vectors dramatically reduced (~50) potentially allowing for in-flight evaluation on traditional processor architectures.

3. CONCLUSIONS

We have presented results of 4 near-real-time products aimed at providing useful and timely information for managing agencies from L-band Polarimetric SAR data. The simple repeat pass composite image would require knowledge for interpretation and onboard storage, however it has shown to be useful at least for fire-damage assessment. Our surface water extent algorithm shows useful accuracy as compared to NLCD2001 over the everglades; its inaccuracies due to wind action on surface roughening are left to be investigated as problematic for actual

flooding scenarios. Of our support vector machine classifiers, the vegetation classifier requires significant processing and provides inaccurate results based on NLCD2001 but hints at better results through higher fidelity ground-truth, while the snow and ice classifier shows good results thus far on our limited set of data.

4. REFERENCES

- DESDynI JPL homepage, 2011, “desdyni: Mission Concept,” <http://desdyni.jpl.nasa.gov/mission/>
- Y. Lou, S. Chien, D. Clark, J. Doubleday, 2010, “Onboard Radar Processing Concepts for the DESDynI Mission”, http://esto.nasa.gov/conferences/estf2010/papers/Lou_DESDynI_ESTF2010.pdf
- Jet Propulsion Laboratory (JPL) 2010, “UAVSAR - Home”, <http://uavsar.jpl.nasa.gov/>
- NASA image created by Jesse Allen, using data provided courtesy of NASA/GSFC/METI/ERSDAC/JAROS, and U.S./Japan [ASTER Science Team](http://earthobservatory.nasa.gov/ASTER_Science_Team). Caption by Holli Riebeek <http://earthobservatory.nasa.gov/IOTD/view.php?id=40118>
- USDA Forest Service, ANGELES NF - STATION FIRE Burned Area Emergency Response · BAER Implementation FREQUENTLY ASKED QUESTIONS Last Updated: 11.04.2009 http://www.fs.usda.gov/Internet/FSE_DOCUMENTS/fsbdev3_020019.pdf
- U.S. EPA, Multi-Resolution Land Characteristics Consortium 2011 (MLRC) “2001 National Land Cover Data (NLCD 2001)” <http://www.epa.gov/mrlc/nlcd-2001.html>
- Pascale C. Dubois, Jakob van Zyl, and Ted Engman, “Measuring Soil Moisture with Imaging Radars,” IEEE TRANSACTIONS ON GEOSCIENCE AND REMOTE SENSING, VOL. 33, NO. 4, JULY 1995 915
- B. Tang and D. Mazzoni, “Multiclass reduced-set support vector machines,” In Proceedings of the 23th International Conference on Machine learning, pages 921–928, New York, NY, USA, 2006. ACM Press.
- K. L. Wagstaff, M. Kocurek, D. Mazzoni, B. Tang, “Progressive Refinement for Support Vector Machines,” Data Mining and Knowledge Discovery, 20(1):53-69, doi:10.1007/s10618-009-0149-y, January 2010.

ACKNOWLEDGEMENT

Portions of this work were performed by the Jet Propulsion Laboratory, California Institute of Technology, under contract from the National Aeronautics and Space Administration.